© 1999 Nature America Inc. • http://neurosci.nature.com

Timing of cochlear feedback: spatial and temporal representation of a tone across the basilar membrane

K. E. Nilsen and I. J. Russell

School of Biological Sciences, University of Sussex, Falmer, Brighton, BN1 9QG, UK
Correspondence should be addressed to I.J.R. (I.J.Russell@sussex.ac.uk)

Electromotile outer hair cell (OHC) feedback provides the sensitivity and sharp frequency tuning of the cochlea. Basilar membrane displacements in response to characteristic frequency (CF) tones were measured with an interferometer at up to 15 locations across the basilar membrane width in the basal turn of the guinea pig cochlea. For CF tones, basilar membrane vibrations were largest beneath the OHCs; these phase-led vibrations beneath outer pillar cells and adjacent to the spiral ligament by ~90°. *Post mortem,* responses measured beneath the OHCs were reduced by up to 65 dB, and the basilar membrane moved with similar phase across its entire width. We suggest OHCs amplify basilar membrane responses to CF tones when the basilar membrane moves at maximum velocity.

© 1999 Nature America Inc. • http://neurosci.nature.com

The basilar membrane of the cochlea vibrates in response to sounds and separates their frequency components as a tonotopic array to the inner (IHC) and outer hair cells distributed along its length[1]. Vibrations deflect morphologically and functionally polarized hair cell sensory bundles; displacements toward the tallest row of stereocilia result in hair cell depolarization[2]. Each section of the basilar membrane responds most sensitively to its characteristic frequency; CFs progress from low at the apex to high at the base of the cochlea. Basilar membrane responses to low-level tones at and near the CF are amplified. For sound levels above about 40 dB SPL (sound pressure level, dB re 2×10^{-5} Pa), responses are compressed, allowing representation of the dynamic range of cochlear responses within the scope of the auditory nerve fiber's neural signaling[3–6]. Electromotile OHCs[7–10] of the organ of Corti are thought to contribute to amplification in the cochlea[11,12] on a cycle-by-cycle basis[13]. In the basal turn of the guinea pig cochlea, precise frequency tuning of the basilar membrane is reflected in the voltage responses of the OHCs to tones[14]. These voltage responses are believed to control OHC electromotility[15], and hence, electromechanical feedback to the cochlear partition for frequencies close to the CF. Acoustic distortion measurements[16,17] and, more directly, specific basilar membrane lesions[18] and measurements of the longitudinal distribution of basilar membrane vibrations to tones of a single frequency[19] indicate that OHCs located near the CF position contribute to local basilar membrane tuning, and, for high-level tones, less than 400 OHCs are actively involved over 1.2 mm. However, it is unclear how transverse motions of the basilar membrane translate into radial shear displacements of the OHC sensory bundles, or at what phase of basilar membrane vibration the cochlear partition receives OHC feedback.

In a simple model of hair cell excitation[20], the basilar membrane hinges about its attachment to the spiral lamina. If the basilar membrane is displaced toward the scala media, stereocilia in the hair bundles are displaced in the excitatory direction, toward the tallest row, through shear displacement between the tectorial membrane and the reticular lamina (Fig. 1a). In excised cochlea, electrical depolarization of the OHCs, as would be caused by excitatory hair bundle displacement, induces a contraction of their cell bodies that draws the basilar membrane and the reticular lamina together[21,22] (Fig. 1b). These findings support[23] and form the basis of[24] mechanical models of basilar membrane tuning comprising two resonant masses, the basilar membrane and the reticular lamina, coupled through the OHCs. For frequency-dependent amplification of basilar membrane displacement, the phase relationship between the basilar membrane and the force produced by the OHCs must be appropriate: amplification will not occur if the two resonant masses move in phase or if OHC forces are delivered in phase with basilar membrane displacement. By leading passive displacement of the basilar membrane by a phase of 90°, force generated by the OHCs would be properly timed to enhance the basilar membrane's motion[23,24]. To deduce when in each vibration cycle OHCs contribute to basilar membrane displacement, we investigated relative movement of different regions across the width of the basilar membrane in response to CF tones (when OHCs are expected to make major contributions), and *post mortem* (when OHCs make no active contribution to the mechanical properties of the basilar membrane[3–6,11,12]).

Results

Tone-evoked basilar membrane displacements were measured with a laser diode interferometer focused to a 5 μm spot with a depth of field of more than 2.3 μm, at up to 15 different locations across the width of the basilar membrane (Fig. 1c). The position of each measurement location was determined with respect to the outer edge of the spiral lamina (0 μm being where the edge of the basilar membrane joins the spiral lamina). These locations were later related to the structural elements of the cochlear partition in histological sections of the measurement site (Fig. 1d). In 9 sensitive preparations from a total of 45 animals, we measured basilar membrane displacement in response to CF tones as func-

© 1999 Nature America Inc. • http://neurosci.nature.com

tions of both sound level and distance from the edge of the spiral lamina. The CF of the measurement location was determined by constructing displacement–level functions (Fig. 2a) for different frequencies and deriving an isoresponse tuning curve (Fig. 2b) from measurements taken 80–100 μm from the spiral lamina. The displacement–level curves saturated, with steeply sloping regions at low and strongly compressed regions at high sound levels. The slope of the steep region was close to unity for frequencies lower than about half an octave below the CF (Fig. 2a, 11 kHz) and became progressively shallower as the frequencies approached and exceeded the CF.

Basilar membrane displacement–level functions in response to CF tones at different recording locations across the width of the basilar membrane are shown for two preparations (Figs. 3a and 4a). The CF of the measurement location was the same (15.5 kHz) in each preparation, but the preparation in Fig. 3 was slightly more sensitive. Magnitude of displacements in response to CF tones varied considerably with location across the width of the basilar membrane. For locations 30–120 μm from the spiral lamina, displacements for any given sound level were at least fourfold larger than those measured 2.5 μm from the edge of the spiral lamina, a distance equal to the laser spot radius. Displacements measured within 30 μm of the spiral ligament were less sensitive and could not be measured above the noise floor of the recording system (0.7 nm, Fig. 3; 0.5 nm, Fig. 4) for sound levels below 40 dB SPL. Within the 30–120 μm region, the low-level slopes (for sound levels below 40 dB SPL) of the displacement–level functions were steeper (0.75–0.8 dB/dB) than those measured close to the spiral lamina (0.5 dB/dB). The slopes of the displacement–level functions from locations close to the spiral ligament could not be measured at sound levels below 40 dB SPL. Therefore, slopes were measured over the range 40–45 dB SPL and were found to be slightly steeper (0.8–1.0) than those measured within the region 30–120 μm from the spiral lamina. At sound levels above 60 dB SPL, compression was greatest for locations within 120 μm of the spiral lamina (0.19–0.21 dB/dB) compared with locations within 70 μm of the spiral ligament (mean, 0.35 dB/dB). Very similar measurements were obtained for seven other preparations. Thus, basilar membrane displacements measured in the immediate vicinity of the OHCs are larger and slightly more compressive than those measured close to the spiral ligament, and therefore farthest from the OHCs.

These differences in displacement–level functions measured across the width of the basilar membrane were revealed in the iso level/gain profiles shown in Figs. 3b and 4b. In these figures, the gain of basilar membrane displacement at constant sound levels was calculated by dividing the displacement by the sound pressure at which the measurement were made and expressing the gain in nm/pascal. The gain for constant sound level CF tones was then expressed as a function of distance across the basilar membrane. The gain peaked at locations 30–50 μm and 80–100 μm from the spiral lamina, which are immediately beneath the organ of Corti (0–120 μm). These locations correspond to the junction between the feet of the inner and outer pillar cells and to the Deiters' cells, respectively; these regions are indicated by solid horizontal bars (Fig. 1d). The peaks are separated by a node of minimum gain at the 60 μm location, near the middle of the outer-pillar-cell foot (horizontal bar, Fig. 1d). In the most-sensitive preparation (Fig. 3b), this node of minimum gain occurred at all sound levels, at least to 90 dB SPL, but disappeared at sound levels above 80 dB SPL in the less-sensitive preparation (Fig. 4b). Vibrations above noise were not detected from the spiral lamina and spiral ligament in

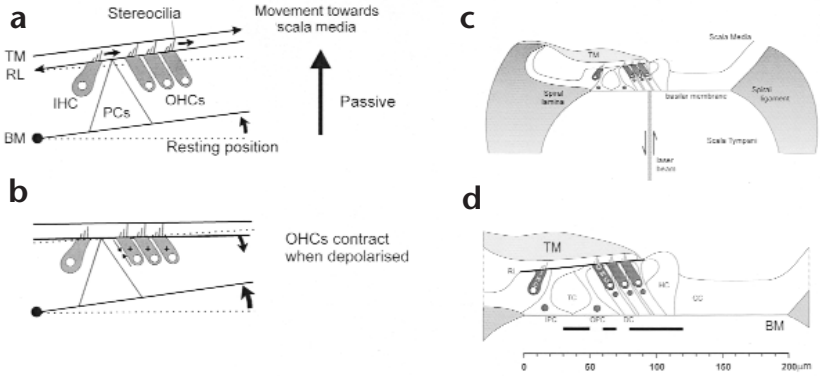

Fig. 1. Cochlear structure and function. **(a)** Model of hair cell excitation without OHC motility according to Davis's theory[20] (see text). **(b)** When depolarized, OHCs contract and draw together the basilar membrane and reticular lamina[21,22]. TM, tectorial membrane; RL, reticular lamina; basilar membrane, basilar membrane; IHC, inner hair cell; OHC, outer hair cell; PCs, pillar cells. **(c)** Experimental arrangement with laser diode beam. **(d)** Diagram of a transverse section through the organ of Corti in the 15.5 kHz region based on measurements made *in vivo* and from histological sections; scale bar referenced to the bony edge of the spiral lamina. Solid horizontal bars indicate the following regions across the basilar membrane width with respect to the bony edge of the spiral lamina: 30–50 μm (junction of inner and outer pillar cells), 60–70 μm (near midpoint of outer pillar cell base), 80–120 μm (Deiters' cells). BM, basilar membrane; TM, tectorial membrane; IHC, inner hair cell; OHC, outer hair cell; HC, Henson cell; CC, Claudius cell region; IPC, inner pillar cell; OPC, outer pillar cell; DC, Deiters' cell; RL, reticular lamina; TC, tunnel of Corti.

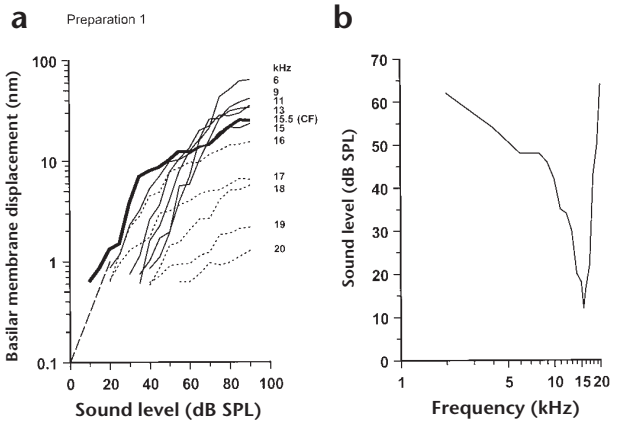

Fig. 2. Relationship of sound pressure level to basilar membrane displacement and frequency. **(a)** Basilar membrane displacement as a function of sound level for tones at frequencies between 6–20 kHz recorded from the 15.5 kHz place in the basal turn of the guinea pig cochlea. Solid lines, below CF; thick line, at CF; dotted lines, above CF. Dashed line indicates slope of one. **(b)** Isoresponse tuning curve derived from the displacement–level functions in **(a)**. Response criterion, 0.7 nm, the basilar membrane displacement at the detection threshold of the compound action potential (CAP) for a 15.5 kHz tone.

© 1999 Nature America Inc. • http://neurosci.nature.com

© 1999 Nature America Inc. • http://neurosci.nature.com

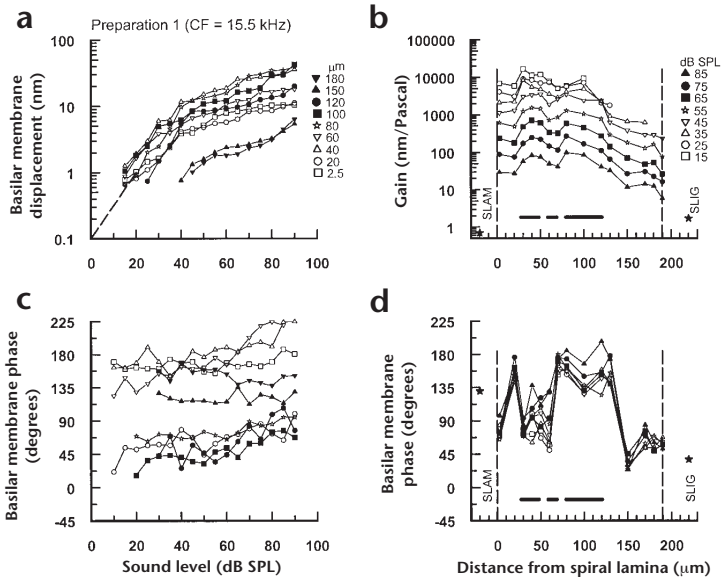

Fig. 3. Preparation 1. **(a)** Basilar membrane displacement-level functions in response to 15.5 kHz (CF) tones for different locations across the width of the basilar membrane. The locations are measured from the edge of the spiral lamina and are indicated by the symbols shown. Dashed line indicates slope of one. For locations 30–120 μm from the spiral lamina and sound levels <40 dB SPL, slopes = 0.81 ± 0.04 dB/dB. For locations 0–120 μm from the spiral lamina and sound levels >60 dB SPL, slopes = 0.19 ± 0.02 dB/dB. For locations within 70 μm of the spiral ligament and sound levels >60 dB SPL, slopes = 0.35 ± 0.03 dB/dB. **(b)** Basilar membrane gain (nm per Pascal, derived from displacement–level functions) in response to 15.5 kHz (CF) tones as a function of measurement location across the width of the basilar membrane for stimulus levels between 15 and 85 dB SPL (indicated by symbols). The vertical dashed lines represent the inner spiral lamina attachment (SLAM) and outer spiral ligament attachment (SLIG) of the basilar membrane. The solid stars represent basilar membrane gain of vibrations measured on the spiral lamina attachment (0.7) and spiral ligament attachment (1.7) at 95 dB SPL in preparation 3 (**Fig. 5**). **(c)** Basilar membrane phase as a function of the stimulus level of 15.5 kHz (CF) tones for different measuring locations across the width of the basilar membrane from the edge of the spiral lamina, indicated by symbols in **(a)**. **(d)** Basilar membrane phase in response to 15.5 kHz (CF) tones as a function of measurement location across the width of the basilar membrane for stimulus levels between 15 and 85 dB SPL (see symbols in **b**). Vertical dashed lines as in **(b)**; the solid stars represent basilar membrane phase of vibrations measured on the spiral lamina attachment and spiral ligament attachment at 95 dB SPL in preparation 3 (**Fig. 5**). Bars in **(b)** and **(d)** as in Fig. 2b; basilar membrane width, 190 μm; CAP threshold at CF, 12 dB SPL; 0 dB loss after opening cochlea to expose the basilar membrane; measurement noise floor 0.7 nm.

response to CF tones of 90 dB SPL or below, but were present for higher sound levels. Gains (spiral lamina, 0.7; spiral ligament, 1.2; Figs. 3b and 4b) were calculated from measurements made on the spiral lamina and the spiral ligament 20 μm from the edge of the basilar membrane at sound levels above 90 dB SPL in a *post-mortem* preparation (Fig. 5). Assuming that the spiral lamina is stiff up to the point where it joins the basilar membrane, then, for low-level tones, responses can differ between the spiral lamina and a point on the basilar membrane 2.5 μm away by 80 dB (see Fig. 3). However, angular rotation of the basilar membrane at its junction with the spiral lamina is very small. Basilar membrane vibrations to a 90 dB SPL, CF tone are about 10 nm when measured at a location 2.5 μm from the spiral lamina. Hence, the displacement gradient from the edge of the spiral lamina to the measuring point is about 1:250, an angular displacement of 0.23 degrees.

To see how different regions across the width of the basilar membrane move in relation to one another in response to CF tones, we measured the phase of basilar membrane displacement relative to the stimulus tone as a function of both measurement

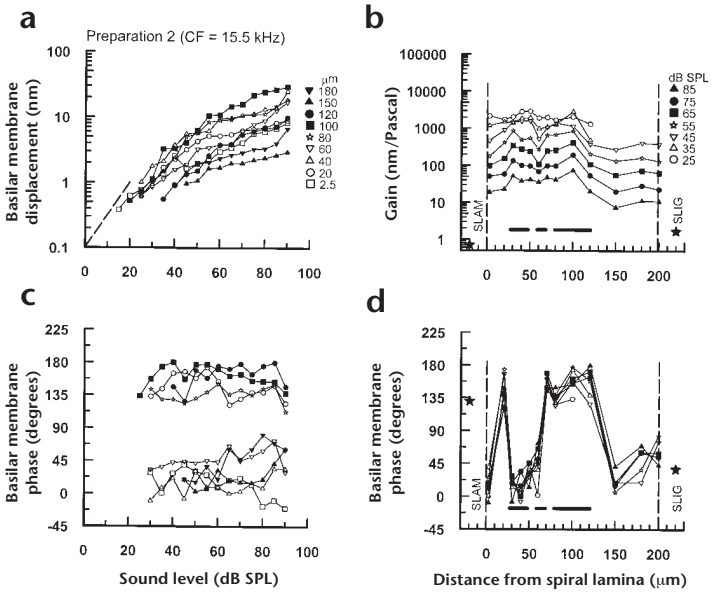

Fig. 4. Preparation 2. **(a)** Basilar membrane displacement–level functions in response to 15.5 kHz (CF) tones for different locations across the width of the basilar membrane. The locations are measured from the edge of the spiral lamina and are indicated by the symbols shown. Dashed line indicates slope of one. For locations 30–120 μm from the spiral lamina and sound levels <40 dB SPL, slopes = 0.75 ± 0.05 dB/dB. For locations 0–120 μm from the spiral lamina and sound levels >60 dB SPL, slopes = 0.21 ± 0.03 dB/dB. For locations within 70 μm of the spiral ligament and sound levels >60 dB SPL, slopes = 0.35 ± 0.03 dB/dB. **(b)** Basilar membrane gain in response to 15.5 kHz (CF) tones as a function of measurement location across the width of the basilar membrane for stimulus levels of 25–90 dB SPL (indicated by symbols). **(c)** Basilar membrane phase as a function of the stimulus level of 15.5 kHz (CF) tones for different measuring locations across the width of the basilar membrane from the edge of the spiral lamina; see symbols in **(a)**. **(d)** Basilar membrane phase in response to 15.5 kHz (CF) tones as a function of measurement location across the width of the basilar membrane for stimulus levels between 25 and 85 dB SPL; see symbols in **(b)**. Vertical dashed lines, stars and horizontal bars in **(b)** and **(d)** as in Fig. 3. Basilar membrane width, 200 μm; CAP threshold at CF, 16 dB SPL; 5-dB loss after opening cochlea to expose the basilar membrane; measurement noise floor, 0.5 nm.

© 1999 Nature America Inc. • http://neurosci.nature.com

© 1999 Nature America Inc. • http://neurosci.nature.com

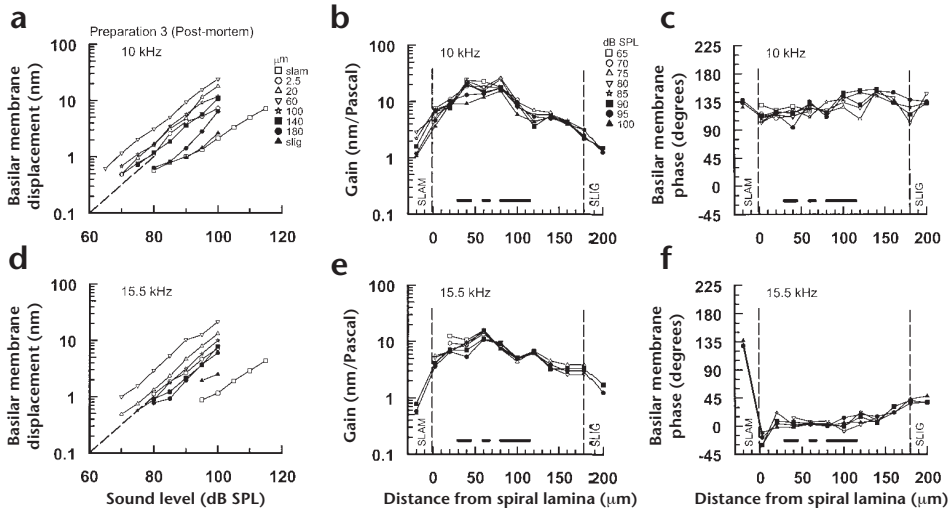

Fig. 5. Preparation 3. Measurements made 1.5–4 h *post mortem* near the 15.5 kHz location on the basilar membrane. **(a)** Displacement–level functions in response to 10 kHz tones for different measuring locations across the width of the basilar membrane. The locations are measured from the edge of the spiral lamina and are indicated by the symbols shown. Dashed line indicates slope of one. **(b)** Basilar membrane gain in response to 10 kHz tones as a function of measurement location across the width of the basilar membrane for stimulus levels of 65–100 dB SPL (indicated by the symbols). **(c)** Basilar membrane phase in response to 10 kHz tones as a function of measurement location across the width of the basilar membrane for stimulus levels of 65–100 dB SPL, indicated by the symbols in **(b)**. **(d)** Displacement–level functions in response to 15.5 kHz tones for different measuring locations across the width of the basilar membrane from the edge of the spiral lamina, indicated by the symbols in **(a)**. Dashed line indicates slope of one. **(e)** Basilar membrane gain in response to 15.5 kHz tones as a function of measurement location across the width of the basilar membrane for stimulus levels of 65–100 dB SPL, as indicated by the symbols in **(b)**. **(f)** Basilar membrane phase in response to 15.5 kHz tones as a function of measurement location across the width of the basilar membrane for stimulus levels of 65–100 dB SPL; see symbols in **(b)**. Vertical dashed lines and horizontal bars in **(b, c, e** and **f)** as in Fig. 4. Basilar membrane width, 180 μm; measurement noise threshold, 0.5 nm.

location and sound level. The phase-level functions (Figs. 3c and 4c) were re-expressed to show the variation of phase with distance from the spiral lamina at different stimulus levels (Figs. 3d and 4d). These plots show similar phases at the attachment to the spiral lamina, beneath the outer pillar cell foot and close to the spiral ligament. In these preparations, the basilar membrane regions beneath the inner-pillar-cell foot and the Deiters' cells may lead the phase of the remainder of the basilar membrane by 135°. Similar findings were obtained in another seven sensitive preparations. In all nine preparations, the greatest variation in phase (90°–180°) occurred between the Deiters' cell region and the outer-pillar-cell foot. Phase measurements from the spiral lamina and spiral ligament in Figs. 3d and 4d were measured from the *post-mortem* preparation shown in Fig. 5.

By measuring the responses to 15.5 kHz and 10 kHz tones in a *post-mortem* preparation from a location close to the 15.5 kHz place, active processes contributing to basilar membrane vibrations were removed. The basilar membrane was relatively insensitive to tones, and displacement responses could only be detected above noise (0.5 nm) when the tone level was increased above 65 dB SPL. The displacement–level slopes approached unity and did not saturate, regardless of the measurement location and frequency (Fig. 5a and d). Basilar membrane vibrations in response to 10 kHz tones were larger than those measured in response to 15.5 kHz tones in the *post-mortem* preparation. Across the width of the basilar membrane, the largest vibrations, and hence, highest gains, were measured beneath the feet of the outer pillar cells (Fig. 5b and e), in contrast to measurements from sensitive preparations in which gains measured beneath the outer pillar cells were smaller than those measured beneath the Deiters' cells (Figs. 3 and 4), but similar to responses of insensitive preparations to high-level tones[25]. Vibrations measured from the spiral ligament

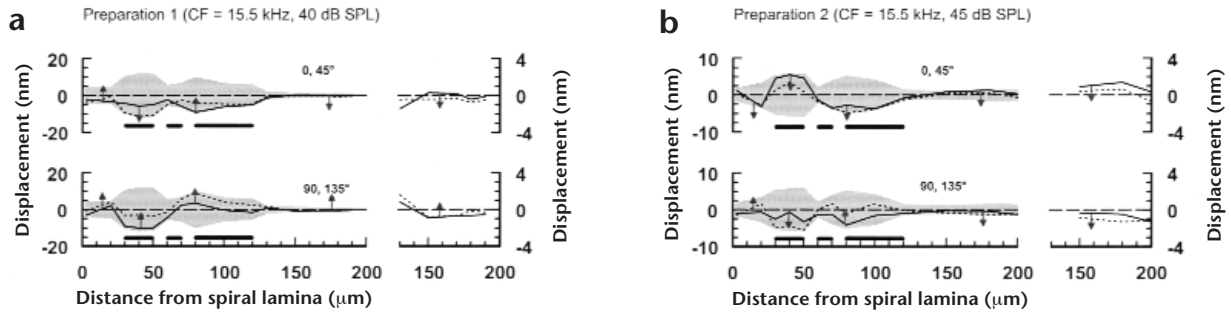

Fig. 6. Basilar membrane displacement as a function of phase and position. **(a)** Preparation 1. Displacement across the width of the basilar membrane as a function of time for a 40 dB SPL tone at the CF (based on data from **Fig. 3**). **(b)** Preparation 2. Displacement across the width of the basilar membrane as a function of time for a 45 dB SPL tone at CF (based on data from **Fig. 4**). The gray shaded area plots the envelope of the basilar membrane displacement. The solid and dotted lines plot the basilar membrane displacement at successive, 45° intervals (0°, solid; 45°, dotted). The arrows indicate the instantaneous direction of basilar membrane motion in the transverse plane; bars as in Fig. 2b. Right column, expanded view of the region from 130 μm to the spiral ligament.

© 1999 Nature America Inc. • http://neurosci.nature.com

© 1999 Nature America Inc. • http://neurosci.nature.com

were in phase with those of the adjacent basilar membrane, indicating that these vibrations were driven by the basilar membrane, or by pressure differences between the scala tympani and scala media. Vibrations measured from the spiral lamina were phase-shifted from those of the adjacent basilar membrane, but were the same for all frequencies measured, an indication that the spiral lamina vibrations are conducted either through the bones of the skull or fluids of the cochlea.

Relative vibration of different regions across the width of the basilar membrane was visualized by plotting the product of the magnitude and cosine of the displacement phase angle (relative to that of the sound source), giving the instantaneous, transverse vector of basilar membrane displacement as a function of location. D*cos[$\theta(t)$] is plotted across the basilar membrane width at two, successive 45°-intervals (solid and dotted lines) for 15.5 kHz CF tones at 40 dB SPL for the sensitive (Fig. 6a) and at 45 dB SPL for the less-sensitive preparation (Fig. 6b), where D is the magnitude of basilar membrane displacement and θ is the phase. In each figure, the gray shaded area, which plots the envelope of the basilar membrane displacement, is widest, and basilar membrane displacement is therefore greatest, between 30–120 μm from the spiral lamina. As shown in Fig. 3b for all sound levels and in Fig. 4b for sound levels below 80 dB SPL, the envelope within the 30–120-μm region is bi-lobed with displacement peaks at the junction between the feet of the inner and outer pillar cells and beneath the Deiters' cells, which are separated by a displacement minimum near the center of the outer pillar cell base. Arrows indicating instantaneous direction of basilar membrane motion show that, as the regions beneath the Deiters' and inner pillar cell moved farthest into the scala tympani or scala media (Fig. 6a and b, upper graphs), the region adjacent to the spiral ligament, driven only indirectly by the OHCs, crossed its resting position and thus moved with maximum velocity.

Discussion

Our measurements show that the basilar membrane beneath the Deiters' cells vibrates in response to CF tones with greater magnitude and with a phase lead of approximately 90° compared to regions beneath outer pillar cell bases and adjacent to the spiral ligament. This complex vibration is absent from a *post-mortem* preparation, which lacks amplification attributable to the OHCs, thereby reducing the gain of basilar membrane vibration in the Deiters' cell region by 66 dB compared with preparation 1 and by 52 dB compared with preparation 2 (Figs. 3, 4 and 5)[26,27]. In contrast to living basilar membrane, all regions across the width of the basilar membrane in the *post-mortem* preparation vibrate in response to CF tones in phase (Fig. 5c and f). *Post mortem*, the largest vibrations occur beneath the outer pillar cells, whereas vibrations beneath the Deiters' cells are similar in magnitude to those measured adjacent to the spiral ligament (Fig. 5b and e). Thus, through their proposed amplification of vibrations of the cochlear partition to frequencies at and around the CF, OHCs produce a particular gain or displacement profile across the width of the basilar membrane. By interacting with other elements in the organ of Corti, OHCs seem to actively suppress outer pillar cell movement but permit other elements, such as Deiters' cells and the junction between the feet of the two pillar cells, to move more freely. Moreover, in sensitive preparations, this displacement profile is preserved at moderate to high sound levels (90 dB SPL), for which basilar membrane vibrations are strongly compressed and the cochlear amplifier approaches its limits. Vibrations in response to CF tones recorded *in vivo* from the region of the basilar membrane adjacent to the spiral ligament are reduced in gain and phase-lag those recorded beneath the Deiters' cells (Figs. 3 and 4). We suggest that forces generated by the OHC directly drive, and may actively stiffen the region of the basilar membrane beneath the Deiters' cells[28–30]. In contrast, governed by its passive mechanical properties, the basilar membrane region adjacent to the spiral ligament merely responds passively to the amplified vibrations from the Deiters' cell region. These observations and proposals may be interpreted in terms of OHC contraction[7–10], when OHCs are depolarized by displacement toward scala media[31], and elongation, when OHCs are hyperpolarized by displacement toward scala tympani. If the remarkable cytoskeletal architecture of the organ of Corti permits OHCs to deliver forces directly to the cochlear partition, then OHCs may boost the vibrations of the basilar membrane by their maximizing changes in length and force generation[32,33] at the time of maximum basilar membrane velocity[23,24].

In common with recent measurements of basilar membrane motion, the basilar membrane vibrations reported here increase slowly in magnitude with increasing sound level above ~40 dB SPL (show compression) in response to tones with frequencies surrounding the CF[12,26,27]. Thus, OHCs seem to be capable of influencing the mechanical properties of the cochlear partition at high stimulus levels, at least for brief periods[12,34]. Signs of amplification and compression are reduced in preparations with depressed sensitivity to sound. Responses measured in the outer pillar cell foot region of the less-sensitive preparation shown were more linear for sound levels above 80 dB SPL than those measured in the more-sensitive preparation (Fig. 4b). As a consequence, the node of minimum vibration at the foot of the outer pillar cell was absent at sound levels above 80 dB SPL; in this respect, but not in terms of phase, vibration patterns resembled those recorded from this region *post mortem* (Fig. 5b and e).

Without a detailed understanding of the mechanical and electrical interaction between individual elements of the cochlear partition, we can only speculate about the basis for the measured 90°–135° phase lead between the basilar membrane beneath the Deiters' cells and that adjacent to the spiral ligament. For example, the 90° phase lead might be a 270° phase delay between OHC depolarization and shortening of the OHC body due to two components. Firstly, a delay of 180° could be introduced if OHC length changes were driven by potentials in the extracellular spaces surrounding the OHCs rather than by intracellular potentials of OHCs themselves[13,35]. An additional 90° delay could be introduced by the resonant properties of the tectorial membrane, which, according to modeling studies[36] and supported by indirect[37] and direct measurements[38], resonates half an octave below the basilar membrane. In many respects, our measurements resemble the behavior of a three-dimensional model of cochlear mechanics[39]. In particular, both the model and our measurements exhibit a bimodal displacement pattern across the width of the basilar membrane. The model also predicts that phase of motion beneath the Deiters' cells leads that of the pillar cells by about 90°. However, in the model, the inner and outer pillar cells are treated as a single element. Thus, the model lacks the more complex phase behavior of the basilar membrane indicated by our measurements, which may result from a flexion point at the junction between the two pillar-cell bases. The model also does not predict our measured phase lead of approximately 90° between the basilar membrane region beneath the Deiters' cells and that adjacent to the spiral ligament. At present, it is impossible to determine whether the 90° phase lead (or 270° delay) was due to the properties of the OHC electromechanical transduction process or to phase delays introduced through vis-

© 1999 Nature America Inc. • http://neurosci.nature.com

© 1999 Nature America Inc. • http://neurosci.nature.com

coelastic interaction between the OHCs and other structural elements of the organ of Corti[40] that might prevent instantaneous transfer of force from OHCs.

We propose a simple model to account for the spatial variation across the width of the basilar membrane in magnitude and phase of the measured displacements in response to CF tones. When the basilar membrane undergoes excitatory displacements toward scala media (Fig. 1), OHCs contract with a lead of 90°, drawing the basilar membrane and the reticular lamina together. According to the model, the outer pillar cell behaves as a rigid strut[40,41] extending from a broad foot via an articulated joint. The outer pillar cell resists the OHC contractions so that, when the basilar membrane is pulled up toward the scala media, the foot of the outer pillar cell rotates slightly and pushes the joint between itself and the inner pillar cell downward toward the scala tympani. The reticular lamina pivots about a fulcrum at the apex of the tunnel of Corti to provide a lever ratio of 4:1 in favor of the OHCs. Upward swings of the proximal edge of the reticular lamina draw up the inner pillar cell, and the region of the basilar membrane immediately underlying it, toward the scala media. The proposed tilting of the reticular lamina upward (as the basilar membrane moves toward and away from the scala media) and downward (as the basilar membrane moves toward and away from the scala tympani) would tend to further amplify shear displacement between the reticular lamina and the tectorial membrane and, hence, amplify the angular rotation of IHC and OHC hair bundles.

Methods

A detailed description of the methods has been published[12]. Recordings were made from deeply anesthetized (0.06 mg atropine sulfate, s.c.; 30 mg per kg pentobarbitone, i.p.; 4 mg per kg Droperidol, i.m.; 1 mg per kg Phenoperidine, i.m.), pigmented guinea pigs (180–300 g). They were tracheotomized and artificially respirated; core temperatures were maintained at 37°C.

The basilar membrane was exposed in the basal turn of the cochlea through an opening into the scala tympani large enough to reveal the insertion of the basilar membrane edges into the inner spiral lamina and the outer spiral ligament (Fig. 1c). Means were taken of 10 consecutive measurements of tone-evoked basilar membrane displacements, made at up to 15 locations across the width of the basilar membrane in the basal turn of the cochlea using the self-mixing effect of a laser diode. The beam of the interferometer was focused to a 5-μm spot on the surface of the basilar membrane. Depth of focus of the beam (d) determined by the numerical aperture (N.A.) of the focusing lens (0.54) and the wavelength of the laser (λ; 670 nm) was given by $d \sim \lambda^2/\text{N.A.}$ and was less than 2.3 μm. The interferometer, attached to a calibrated piezo stack, was calibrated at each measurement location by vibrating it over a known range of displacements. Calibration could be checked against the intrinsic calibration of the interferometer[12]. The measurement noise threshold was obtained in the first 20 ms before the presentation of each tone burst. Micropositioners were used to position the laser spot, and both the width of the basilar membrane and the location of the laser spot were obtained from micrometer readings. After measurements at each location, micrometer readings of the locations of the inner and outer edges of the basilar membrane were confirmed, and measurements at specific locations across the width of the basilar membrane were repeated to check for changes in the measurement conditions. The opening in the cochlear wall was not sealed with a cover glass, but artifacts of tone-driven fluid displacement at the meniscus were not observed at the frequencies and sound levels used in the *in-vivo* experiments. A dental point was placed close to the edge of the opening in the cochlea wall to stabilize the meniscus. If the meniscus changed during the sequence of measurements, thereby altering the view of the basilar membrane, the experiment was recommenced. It was not possible to compensate for the apparent shift in the basilar membrane image through the meniscus. Voltage responses from the interferometer were measured with a two channel lock-in amplifier (Brookdeal 5210), digitized at 2.5 kHz with a Data Translation 2828 data acquisition board. Experimental control, data acquisition and data analysis, including computation of basilar membrane displacement and phase, were performed using a PC with programs written in Asyst (Keithley, Taunton, Massachusetts). Cochlear sensitivity was assessed at each major step in preparation and at regular intervals throughout the experiment by measuring the compound action potential audiogram for 1–30 kHz with a Ag/AgCl electrode at the round window. Pure tone stimuli (40-ms duration with 2-ms cosine-shaped rise and fall times) were delivered to the tympanic membrane every 200 ms by a closed acoustic system, which was calibrated *in situ*. Sound pressure levels are expressed in dB SPL (dB re 2×10^{-5} Pa).

With respect to the apex of the cochlea, the location along the length of the basilar membrane of the recording locations can be determined from the empirical relationship between the CF of the recording location and its position along the length of the cochlea[19,42]. Accordingly, the 15.5 kHz location will be 14.6 mm from the apex of the cochlea, and this was confirmed by making a micropipet lesion at the recording location and then measuring the distance between the apex and the lesion *post mortem*[19]. Histological cross sections were made from cochleae fixed overnight in 2.5% glutaraldehyde, decalcified for 4–6 weeks in 10% EDTA, embedded in Epon and sectioned at 1–2 μm at the basilar membrane displacement measurement site. The site was identified either from a small lesion made in the adjacent spiral lamina at the termination of the measurement or from its relationship to the opening in the wall of the cochlea. Distances between structures were measured using eyepiece and stage graticles. There was close agreement (within 5–10% and attributable to shrinkage during fixation) between basilar membrane width measured during the experiment and that measured from sections. Although there was shrinkage of individual elements within the organ of Corti, there was good agreement between the basilar membrane width and the location of the bases of the pillar cells and Deiters' cells measured from the sections with those measured at the time of recording. These experiments were performed under the authority of Home Office Licence PPL 70/4560.

Acknowledgements

We thank James Hartley for designing and constructing electronic apparatus, Richard Goodyear for help and advice with histology and Thomas Collett, Manfred Kössl, Andrei Lukashkin and Guy Richardson for comments on early drafts of the manuscript. This research was supported by the MRC.

RECEIVED 3 MARCH; ACCEPTED 19 MAY 1999

1. von Békésy, G. in *Experiments in Hearing* 403–634 (McGraw-Hill, New York, 1960).
2. Hudspeth, A. J. How the ear's works work. *Nature* 341, 397–404 (1989).
3. Sellick, P. M., Patuzzi, R. & Johnstone, B. M. Measurement of basilar membrane motion in the guinea pig using the Mössbauer technique. *J. Acoust. Soc. Am.* 72, 131–141 (1982).
4. Robles, L., Ruggero, M. A. & Rich, N. C. Basilar-membrane mechanics at the base of the chinchilla cochlea. 1. Input-output functions, tuning curves, and response phases. *J. Acoust. Soc. Am.* 80, 1364–1374 (1986).
5. Nuttall, A. L., Dolan, D. F. & Avinash, G. Laser Doppler velocitometry of basilar membrane vibration. *Hear. Res.* 51, 203–214 (1991).
6. Cooper, N. P. & Rhode, W. S. Basilar-membrane mechanics in the hook region of cat and guinea-pig cochleae—sharp tuning and nonlinearity in the absence of base-line position shifts. *Hear. Res.* 63, 163–190 (1992).
7. Brownell, W. E., Bader, C. R., Bertrand, D. & de Ribaupierre, Y. Evoked mechanical responses of isolated cochlear outer hair-cells. *Science* 227, 194–196 (1985).
8. Ashmore, J. F. A fast motile response in guinea-pig outer hair-cells - the cellular basis of the cochlear amplifier. *J. Physiol.* (*Lond.*) 388, 323–347 (1987).
9. Dallos, P., Evans, B. N. & Hallworth, R. Nature of the motor element in electrokinetic shape changes of cochlear outer hair-cells. *Nature* 350, 155-157 (1991).
10. Santos-Sacchi, J. On the frequency limit and phase of outer hair cell motility: Effects of the membrane filter. *J. Neurosci.* 12, 1906–1916 (1992).
11. Ruggero, M. A. & Rich, N. C. Furosemide alters organ of Corti mechanics - evidence for feedback of outer hair-cells upon the basilar-membrane. *J.*

© 1999 Nature America Inc. • http://neurosci.nature.com

© 1999 Nature America Inc. • http://neurosci.nature.com

Neurosci. 11, 1057–1067 (1991).
12. Murugasu, E. & Russell, I. J. The effect of efferent stimulation on basilar membrane displacement in the basal turn of the guinea pig cochlea. *J. Neurosci.* 16, 325–332 (1996).
13. Kolston, P. J. A faster transduction mechanism for the cochlear amplifier? *Trends Neurosci.* 18, 427–429 (1995).
14. Russell, I. J., Kössl, M. & Murugasu, E. in *Advances in Hearing Research* (eds. Manley, G. A., Klump, G. M., Köppl, C., Fastl, H., Oeckinghaus, H.) 125–135 (World Scientific, Singapore, 1995).
15. Santos-Sacchi, J. & Dilger, J. P. Whole cell currents and mechanical responses of isolated outer hair cells. *Hear. Res.* 35, 143–150 (1988).
16. Allen, J. B. & Fahey, P. F. Using acoustic distortion products to measure the cochlear amplifier gain on the BM. *J. Acoust. Soc. Am.* 92, 178–188 (1993).
17. Mills, D. M. & Rubel E. W. Development of the base of the cochlea: place code shift in the gerbil. *Hear. Res.* 122, 82–96 (1998).
18. Cody, A. R. Acoustic lesions in the mammalian cochlea: Implications for the spatial distribution of the 'active process'. *Hear. Res.* 62, 166–172 (1992).
19. Russell, I. J. & Nilsen, K. E. The location of the cochlear amplifier: Spatial representation of a single tone on the guinea pig basilar membrane. *Proc. Natl. Acad. Sci. USA* 94, 2660–2664 (1997).
20. Davis, H. Transmission and transduction in the cochlea. *Laryngoscope* 68, 359–382 (1958).
21. Mammano, F. & Ashmore, J. F. Reverse transduction measured in the isolated cochlea by laser Michelson interferometry. *Nature* 365, 838–841 (1993).
22. Mammano, F., Kros, C. J. & Ashmore, J. F. Patch clamped responses from outer hair cells in the intact adult organ of Corti. *Pflügers Arch.* 430, 745–750 (1995).
23. Geisler, C. D. & Sang, C. N. A cochlear model using feedforward outer-hair-cell forces. *Hear. Res.* 86, 132–146 (1995).
24. Markin, V. S. & Hudspeth, A. J. Modelling the active process of the cochlea - phase-relations, amplification, and spontaneous oscillation. *Biophys. J.* 69, 138–147 (1995).
25. Cooper, N. P. & Rhode, W. S. Basilar membrane tonotopicity in the hook region of the cat cochlea. *Hear. Res.* 63, 191–196 (1992).
26. Nuttall, A. L. & Dolan, D. F. Steady-state sinusoidal velocity responses of the basilar membrane in guinea pig. *J. Acoust. Soc. Am.* 99, 1556–1565 (1996).
27. Ruggero, M. A., Rich, N. C., Recio, A., Narayan, S. S. & Robles, L. Basilar membrane responses to tones at the base of the chinchilla cochlea. *J. Acoust. Soc. Am.* 101, 2151–2163 (1997).
28. Allen, J. B. in *Diversity in Auditory Mechanics* (eds. Lewis, E. R. *et al.*) 167–175 (World Scientific, Singapore, 1996).
29. Russell, I. J. & Schauz, C. Salycilate ototoxicity: effects on the stiffness and electromotility of outer hair cells isolated from the guinea pig cochlea. *Aud. Neurosci.* 1, 309–319 (1995).
30. Murugasu, E. & Russell, I. J. Salycilate ototoxicity: the effects on basilar membrane displacement, cochlear microphonics, and neural responses in the basal turn of the guinea pig cochlea. *Aud. Neurosci.* 1, 139–150 (1995).
31. Russell, I. J. & Sellick, P. M. Low-frequency characteristics of intracellularly recorded receptor-potentials of hair cells in the guinea pig cochlea hair cells. *J. Physiol. (Lond.)* 338, 179–206 (1983).
32. Hallworth, R. Passive compliance and active force generation in the guinea pig outer hair cell. *J. Neurophysiol.* 74, 2319–2328 (1995).
33. Frank, G., Hemmert, W. & Gummer, A. W. Limiting dynamics of high-frequency electromechanical transduction of outer hair cells. *Proc. Natl. Acad. Sci. USA* 96, 4420–4425 (1999).
34. Russell, I. J. & Murugasu, E. Medial efferent inhibition of basilar membrane displacement is greatest at moderate to high levels for near CF tones. *J. Acoust. Soc. Am.* 102, 1734–1738 (1997).
35. Dallos, P. & Evans, B. N. High-frequency motility of outer hair cells and the cochlear amplifier. *Science* 267, 2006–2009 (1995).
36. Allen, J. B. Cochlear micromechanics—A physical model of transduction. *J. Acoust. Soc. Am.* 68, 1660–1670 (1980).
37. Brown, A. M., Gaskill, S. A. & Williams, D. M. Mechanical filtering of sound in the inner ear. *Proc. R. Soc. Lond. B Biol. Sci.* 250, 29–34 (1992).
38. Gummer, A. W., Hemmert, W. & Zenner, H. P. Resonant tectorial membrane motion in the inner ear: its crucial role in frequency tuning. *Proc. Natl. Acad. Sci. USA* 93, 8727–8732 (1996).
39. Kolston, P. J. Comparing *in vitro*, *in situ*, and *in vivo* experimental data in a three-dimensional model of mammalian cochlear mechanics. *Proc. Natl. Acad. Sci. USA* 96, 3676–3681 (1999).
40. Tolomeo, J. A. & Holley, M. C. Mechanics of microtubule bundles in pillar cells from the inner ear. *Biophys. J.* 73, 2241–2247(1997).
41. Mogensen, M. M. *et al.* Keratin filament deployment and cytoskeletal networking in a sensory epithelium that vibrates during hearing. *Cell Motil. Cytoskeleton* 41, 138–153 (1998).
42. Greenwood, D. D. A cochlear frequency-position function for several species—29 years later. *J. Acoust. Soc. Am.* 87, 2592–2605 (1990).

© 1999 Nature America Inc. • http://neurosci.nature.com